Journal of Molecular Science

Journal of Molecular Science
Volume 35 Issue 3, Year of Publication 2025, Page 1237-1245
DoI-10.004687/1000-9035.2025.165

Journal of Molecular Science
www.jmolecularsci.com ISSN:1000-9035

Eco-friendly Synthesis and Fabrication of ZnO–MnO_2 Nanocomposite via Pithecellobium dulce Fruit Juice Extract for Hydrazine Sensing Applications

Pradeepa K[1], Shreekanta S. A[2]*, Raghu G. K[3]
Shimoga – 577203, Karnataka, India.

Article Information
Received: 24-10-2025
Revised: 12-11-2025
Accepted: 22-11-2025
Published: 27-12-2025

Keywords
Pithecellobium dulce, active surface area of electrode, sensitivity, reproducibility, anodic peak current, limit of detection (LOD).

ABSTRACT
In this work, we report the eco-friendly synthesis and fabrication of a zinc oxide–manganese dioxide (ZnO–MnO_2) nanocomposite using *Pithecellobium dulce* fruit juice extract as a natural reducing and stabilizing agent. The nanocomposite was prepared through a simple and cost-effective hydrothermal method, followed by calcinations at high temperature to enhance crystallinity.The structural and morphological properties of the synthesized material were characterized using Fourier-transform infrared spectroscopy (FTIR), X-ray diffraction (XRD), scanning electron microscopy (SEM), and energy-dispersive X-ray spectroscopy (EDX). These analyses confirmed the formation of well-dispersed ZnO and MnO_2 nanoparticles with uniform morphology and high surface area. Electrochemical studies were performed using cyclic voltammetry (CV) and amperometry in phosphate buffer solution (PBS, pH 7.4). The ZnO–MnO_2 modified electrode exhibited excellent electro catalytic activity towards hydrazine oxidation, showing a notable reduction in over potential and a significant increase in oxidation current compared to bare and individually modified electrodes. This enhanced performance is attributed to the synergistic interaction between ZnO and MnO_2, which facilitates rapid electron transfer and provides more active sites for hydrazine adsorption and oxidation. The developed sensor demonstrated a wide linear detection range (10 µM to 700 µM), a low detection limit (2.87 µM), high sensitivity (0.376 µA μM^{-1}), and excellent repeatability and reproducibility. Moreover, the electrode showed outstanding selectivity for hydrazine even in the presence of common interfering substances. Stability tests confirmed consistent performance over multiple cycles and extended storage periods.

1. INTRODUCTION:

Hydrazine (N_2H_4) is a low molecular weight inorganic compound known for its high toxicity and strong reducing properties. It is extensively used in various industrial applications, including fuel cells, pharmaceuticals, agrochemicals, and polymer synthesis [1–4]. However, due to its toxic and carcinogenic nature, even trace amounts of hydrazine pose serious risks to both human health and the environment[5,6]. The United States Environmental Protection Agency (EPA) has classified hydrazine as a probable human carcinogen [7]. Therefore, the development of sensitive, selective, and reliable methods for hydrazine detection is critically important [8].Among various analytical techniques, electrochemical sensing has emerged as a promising approach for hydrazine detection due to its simplicity, cost-

Journal of Molecular Science
Journal of Molecular Science
Volume 35 Issue 3, Year of Publication 2025, Page 1237-1245
DoI-10.004687/1000-9035.2025.165

effectiveness, high sensitivity, and real-time monitoring capability [9–12]. The performance of an electrochemical sensor is highly dependent on the electrode material used [13].Nanostructure metal oxide materials such as zinc oxide (ZnO) and manganese dioxide (MnO_2) have attracted significant attention as electrode modifiers because of their excellent catalytic properties, high surface area, and good electron transfer kinetics [14]. ZnO, a wide band gap semiconductor, exhibits strong adsorption capacity and rapid electron transfer capabilities, enhancing its electro catalytic activity [15]. Similarly, MnO_2 is known for its multiple oxidation states and high redox activity, making it highly effective for catalytic oxidation reactions such as hydrazine detection. The combination of ZnO and MnO_2 in a nanocomposite form is expected to synergistically enhance sensitivity, selectivity, and reduce the detection limit of the hydrazine sensor [16]. The present study focuses on the eco-friendly synthesis and evaluation of ZnO/MnO_2 nanocomposite-modified glassy carbon electrodes (GCEs) for electrochemical hydrazine sensing. The influence of these metal oxide nonmaterial's on sensor performance is systematically investigated to explore their potential in real-world applications such as environmental, food, and industrial monitoring [17]. As an effective reducing agent, hydrazine is widely employed in fuel cells, pharmaceutical synthesis, agricultural formulations, and polymer production [18,19]. However, its trace presence in the environment can lead to significant safety concerns. Thus, the rapid, sensitive, and selective detection of hydrazine is essential for protecting human health and the ecosystem [20]. Electrochemical detection techniques are particularly appealing due to their portability, affordability, and real-time monitoring capabilities. The key challenge lies in selecting an electrode material that exhibits high catalytic activity, efficient electron transfer, and resistance to fouling. In this context, ZnO/MnO_2 modified GCEs represent a promising and efficient platform for hydrazine detection [21,22].

2.0 Experimental Section:

2.1Chemicals and Reagents:

Zinc chloride ($ZnCl_2$) was purchased from Thomas Baker Chemicals Pvt. Ltd. Manganese (II) chloride tetra hydrate ($MnCl_2{\cdot}4H_2O$) was obtained from Merck Life Science Pvt. Ltd. Hydrazine hydrate ($N_2H_4{\cdot}H_2O$, 80%) was supplied by S.D. Fine Chem. Ltd. Potassium ferrocyanide ($K_4[Fe(CN)_6]$), potassium chloride (KCl), and phosphate buffer components (NaH_2PO_4 and Na_2HPO_4) were procured from Fisher Scientific. All chemicals were of analytical grade and used without further purification. Deionized water was used for the preparation of all solutions.

The Pithecellobium dulce fruit was collected from Kodi Muddanahalli, Murarji Desai Residential PU College, Tumkur District, Karnataka, India.

2.2 Preparation of *Pithecellobium dulce* Extract

Fresh, ripe Pithecellobium dulce fruit peels were manually separated from the seeds and dried under shade for one week. The dried peels were then ground into a fine powder using a mortar and pestle. About 12 grams of the powder were dissolved in 100 ml of deionized water and boiled for 1 hour at 60 °C. The resulting mixture was filtered using Whatman filter paper, and the filtrate was stored at 4 °C for further use as a natural reducing and stabilizing agent.

2.3 Synthesis of ZnO/MnO_2 Nanocomposite

The ZnO/MnO_2 nanocomposite was synthesized via a hydrothermal method. initially 0.44 g of $ZnCl_2$ was dissolved in 50 mL of deionized water, and 0.4 g of $MnCl_2{\cdot}4H_2O$ was dissolved in 50 ml D.I water seperately. Both solutions were mixed in an Erlenmeyer flask and stirred magnetically for 20 minutes. Then, 60 mL of the prepared *Pithecellobium dulce* extract was added to the mixture, and stirring continued for an additional 30 minutes. Subsequently, 2 M NaOH was added dropwise until the pH of the solution reached approximately 10. The mixture was then subjected to hydrothermal treatment by heating at 85 °C for 4.5 hours. A brownish precipitate was formed, which was collected by centrifugation and washed thoroughly with ethanol followed by deionized water to remove impurities.The precipitate was dried at 80 °C overnight and then calcined at 400 °C for 3.5 hours to obtain crystalline ZnO/MnO_2 nanoparticles.

Graphical abstract:-

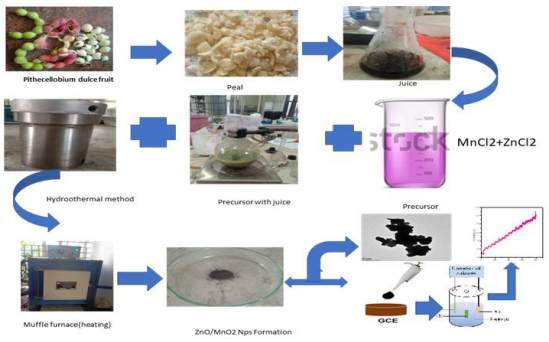

Fig.1 Shows the graphical abstract of synthesis of ZnO/MnO_2 Nanocomposite.

3.0 Materials Characterization:

Fourier-transform infrared spectroscopy (FT-IR; PerkinElmer) was used to analyze the functional groups present in the synthesized nanocomposite.

Journal of Molecular Science
Journal of Molecular Science
Volume 35 Issue 3, Year of Publication 2025, Page 1237-1245
DoI-10.004687/1000-9035.2025.165

The spectra were recorded in the range of 400–4000 cm^{-1} using KBr as a dispersing medium.Powder X-ray diffraction (XRD) patterns were obtained using an X'Pert Explorer PANalytical diffractometer equipped with CuKα₁ radiation (λ = 1.5406 nm), operated at 40 kV and 35 mA. This analysis was conducted to determine the crystalline phases and structural features of the ZnO/MnO_2 nanocomposite.The surface morphology of the synthesized ZnO/MnO_2 nanoparticles was examined using field-emission scanning electron microscopy (FE-SEM; JSM-7600F, Japan). Elemental composition and mapping were carried out using energy-dispersive X-ray spectroscopy (EDS; JEOL, Japan).Further structural evaluation at the nanoscale was performed by transmission electron microscopy (TEM; JEM-2100F, Japan). TEM samples were prepared by dispersing the nanoparticles in ethanol, followed by ultrasonication. A drop of the suspension was placed on a carbon-coated copper grid and dried at room temperature before imaging.

3.1 Electrode Fabrication and Electrochemical Evaluation:

A glassy carbon electrode (GCE, diameter 0.071 cm^2) was used as the base for sensor fabrication. The electrode surface was polished sequentially with alumina slurries of 1.0 µm, 0.3 µm, and 0.05 µm, followed by thorough rinsing with ethanol and deionized water. The cleaned electrode was dried under a nitrogen stream.A dispersion of ZnO/MnO_2 nanocomposite was prepared by mixing 2 mg of the powder in 2 mL of deionized water containing 0.1% Nafion (used as a binder). The mixture was ultrasonicated for 30 minutes to obtain a stable suspension. An aliquot of 4 µL of this suspension was drop-cast onto the surface of the pre-treated GCE and allowed to dry at room temperature, forming the modified electrode (ZnO/MnO_2/GCE).

3.2 Electrochemical Analysis:

Electrochemical measurements were carried out using a CHI6155E electrochemical workstation (CH Instruments, USA) employing a standard three-electrode configuration: the ZnO/MnO_2-modified GCE as the working electrode, an Ag/AgCl (1 M KCl) reference electrode, and a platinum wire as the counter electrode.All electrochemical experiments were conducted in 0.1 M phosphate buffer solution (PBS) at pH 7.4, maintained at room temperature. Cyclic voltammetry (CV) was performed in the potential range of –1.0 V to +1.0 V at various scan rates to evaluate the redox behavior and electrocatalytic activity.Amperometric detection of hydrazine was conducted by stepwise addition of hydrazine (ranging from 20 µM to 400 µM) into a continuously stirred PBS solution, with the working electrode poised at an applied potential of +0.48 V. The resulting current responses were recorded to evaluate the sensitivity and linear response range of the sensor.

4.0 RESULTS AND DISCUSSION:

4.1 Materials Characterization FT-IR and XRDAnalysis:

Fourier-transform infrared (FTIR) spectroscopy was used to investigate the structural and functional groups present in the synthesized nanocomposite within the spectral range of 400–4000 cm^{-1} using. The FTIR spectra of ZnO/MnO_2 nanocomposites are shown in Fig(2).The Characteristic absorption bands observed at 530 cm^{-1} and 700 cm^{-1} correspond to the stretching vibrations of Zn–O**,** Mn–O, respectively and the peak at 3200-3500 **cm^{-1}** for the stretching vibration of O-H in water and peak at 1500 **cm^{-1}** and 3000 **cm^{-1}** is the stretching vibration of C-O [23]. all these confirming the formation of the metal oxide nanocomposite .

The crystallographic structure of the ZnO/MnO_2 nanocomposite was analyzed using XRD The diffraction pattern, shown in Fig(3), exhibits highly intense and sharp peaks at 2θ values of **31.76°, 34.11°, 39.42°, 47.51°, 56.55°, 62.84°, 67.90°, 69.84°, 76.86°, 82.11°, and 88.55°,** corresponding to the (100), (002), (101), (102), (110), (103), (112), (201), (202) ,(104) and (203) diffraction planes respectively. These values closely match the standard diffraction data from JCPDS card No. 01-078-4498 [24] confirming the presence of crystalline ZnO and MnO_2 composite nano material has cubic and hexagonal crystal shape.

The calculated average crystallite size of the nano composite was determined using the Debye–Scherrer equation:

$$D = K\lambda/\beta cos\theta$$

λ (1.54 Aº) → wavelength of X-ray incident beam .

β → full width at half maximum of the diffraction of peak .

Θ→Bragg's diffraction angle

K(0.91)→ Scherer's constant

Using this formula, the average crystallite size was estimated to be 0.419 **nm.**

Journal of Molecular Science
Journal of Molecular Science
Volume 35 Issue 3, Year of Publication 2025, Page 1237-1245
DoI-10.004687/1000-9035.2025.165

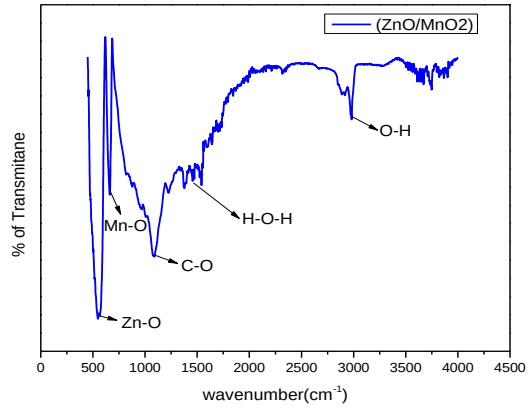

Fig.2 Shows the FTIR spectra of ZnO/MnO_2 NPs.

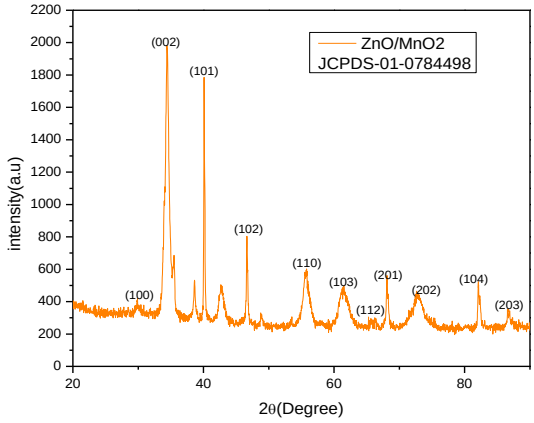

Fig.3 shows the Powder XRD of ZnO/MnO_2 NPs.

SEM with EDAX and TEM Analysis:

FE-SEM is the prominent method to study The morphology of synthesized material. ZnO/MnO_2 nanocomposite was observed using field-emission scanning electron microscopy (FE-SEM, JSM-7600F, Japan). Fig.4 (a-c) shows the SEM image, which reveals that the nanoparticles are uniformly distributed with a relatively porous and agglomerated surface structure, suitable for electrochemical applications due to the enhanced surface area.The corresponding energy-dispersive X-ray spectroscopy (EDS) analysis, shown in Fig.4 (d), confirms the presence of elemental Zn, Mn, and O in the composite with small amount of Carbon as impurity, it indicating successful synthesis and purity of the ZnO/MnO_2 nanocomposite.

Transmission electron microscopy further revealed the detailed internal structure and particle morphology of the nanocomposite. The image shown in Fig. (5) demonstrates the crystalline nature of the ZnO/MnO_2 nanoparticles with an interplanar spacing of approximately **0.219 nm,** supporting the XRD results. The particles exhibited mixed cubic and hexagonal shapes, confirming the formation of a composite structure.

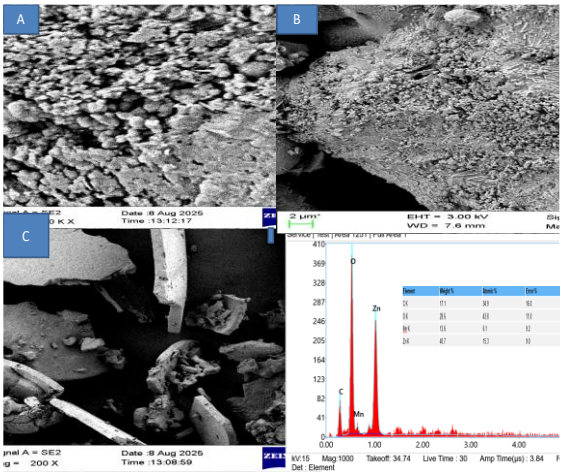

Fig.4.FESEM images of ZnO/MnO_2 nanomaterials(A-C) low to high magnified images and (d) represents the EDAX of ZnO/MnO_2 nanoparticles With elemental analysis.

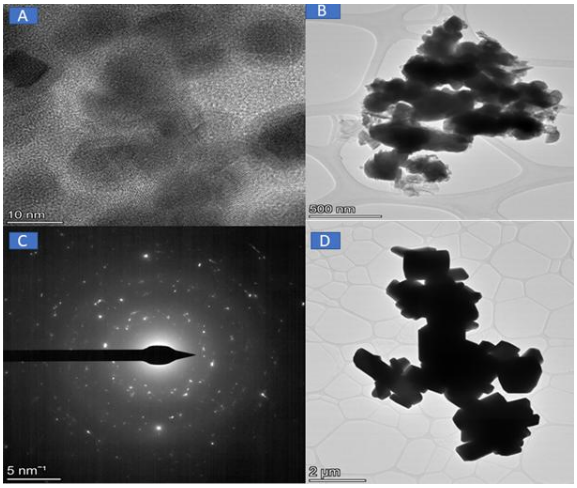

Fig.5.HR-TEM images of ZnO/MnO_2 nanomaterials(A-D) different magnified images and of ZnO/MnO_2 nanoparticles.

4.2 Electrochemical Behavior of ZnO/MnO_2/GCE Modified Electrodes

Cyclic voltammetry (CV) studies were conducted to investigate the electrocatalytic performance of the modified electrodes using various configurations, bare GCE, ZnO/GCE, MnO_2/GCE, and ZnO/MnO_2/GCE, both in the absence and presence of hydrazine. Measurements were carried out in 0.1 M phosphate buffer solution (PBS 0.1M,pH 7.4).**In the Absence of Hydrazine**As shown in Fig. (6), the CV responses of the electrodes in PBS without hydrazine exhibited minimal or no anodic peak current, especially for the bare GCE and slightly modified electrodes. This indicates that the electrode materials

Journal of Molecular Science
Volume 35 Issue 3, Year of Publication 2025, Page 1237-1245
DoI-10.004687/1000-9035.2025.165

themselves have negligible redox activity in the absence of the analyte.similarly **in the Presence of 0.1M PBS P^H 7.4** upon the addition of hydrazine (10 µM), significant changes were observed Fig. (7) the **bare GCE** showed no distinct oxidation peak, indicating poor electrocatalytic activity.The **ZnO/GCE** and **MnO_2/GCE** exhibited notable oxidation peaks at approximately +0.48V potential range with anodic peak currents (Ipa) of **25.02 µA** and **15.72 µA**, respectively.The **ZnO/MnO_2/GCE** displayed a highly enhanced and sharper oxidation peak at **32.91V**, with a significantly higher Ipa of **7.91 µA**.This considerable enhancement in the anodic peak current for ZnO/MnO_2/GCE suggests improved electron transfer kinetics and an increased number of active sites, attributed to the synergistic effect between ZnO and MnO_2 in the composite. The porous morphology and high surface area also contribute to the increased electrocatalytic response.

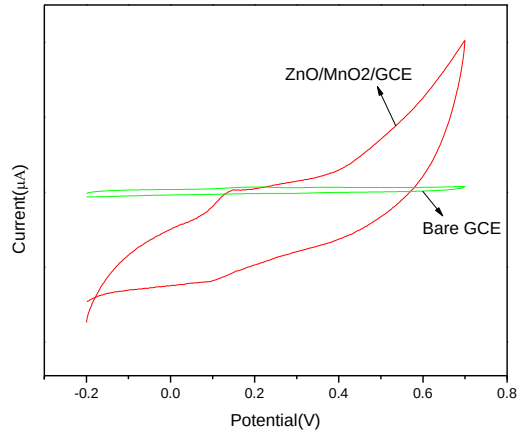

Fig.6.Shows Graph of Bare GCE and ZnO/MnO_2 modified GCE in 0.1M PBS (P^H 7.4)at scan rate of 50mvmvs^{-1}.

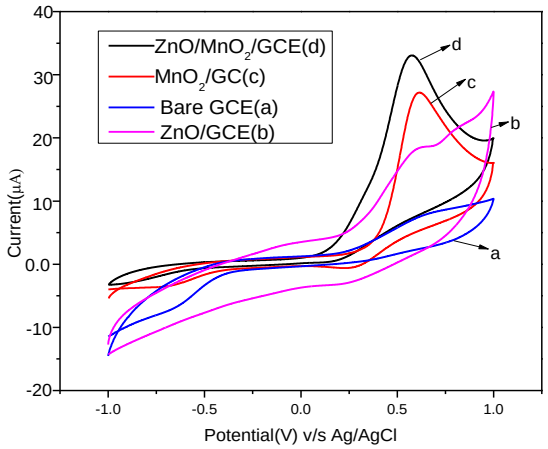

Figure 7. depicts the graph of (a)bare GCE (b) ZnO modified GCE (c)MnO_2 modified GCE (d) ZnO/MnO_2 modified GCE in the presence of 10µM of hydrazine with 0.1M PBS(P^H 7.4)at a scan rate of 50 mvs^{-1}.

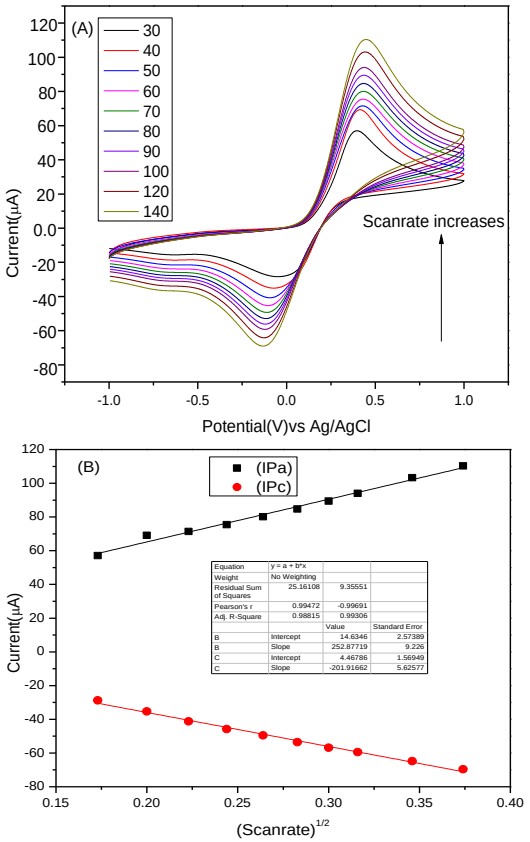

Fig (8) (A)CV responses at 0.1M KCl with 0.5M $K_4[Fe(CN)_6]$ on Modified ZnO/MnO_2/GCE for different scanrates varies from 30 to 120 mVs^{-1}.(B)Relationship between IPa and IPc vs squareroot of scanrate.

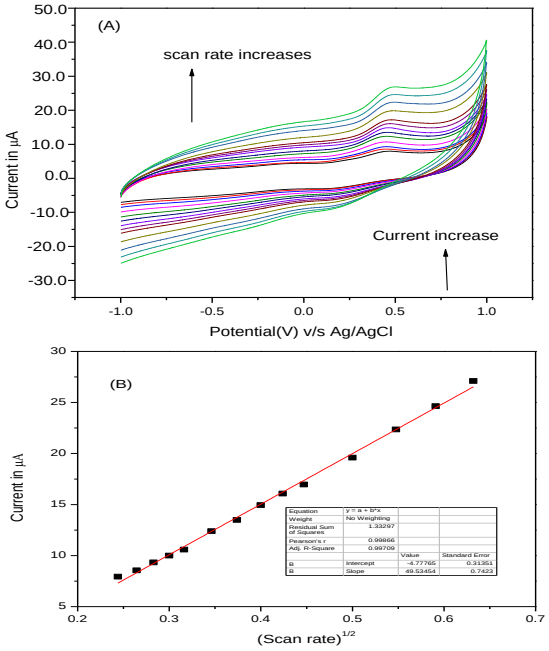

Fig.9(A)cyclic voltammograms of modified ZnO/MnO_2 GCE measurement in 0.1M PBS (P^H 7.4) for 10µM Hydrazine for different scan rate 20 to 120 mvs^{-1}.(B) plot of peak current v/s (Scanarate)$^{1/2}$

Journal of Molecular Science
Journal of Molecular Science
Volume 35 Issue 3, Year of Publication 2025, Page 1237-1245
DoI-10.004687/1000-9035.2025.165

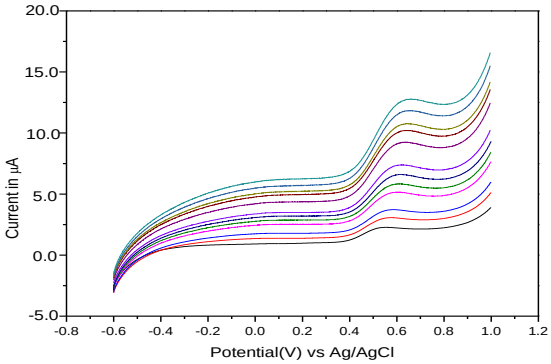

Fig .10.(A)Linear sweep voltammograms of ZnO/MnO_2 modified GCE measurement in 0.1M PBS(P^H 7.4) containing 10µM Hydrazine at different scan rate (mvs^{-1}).

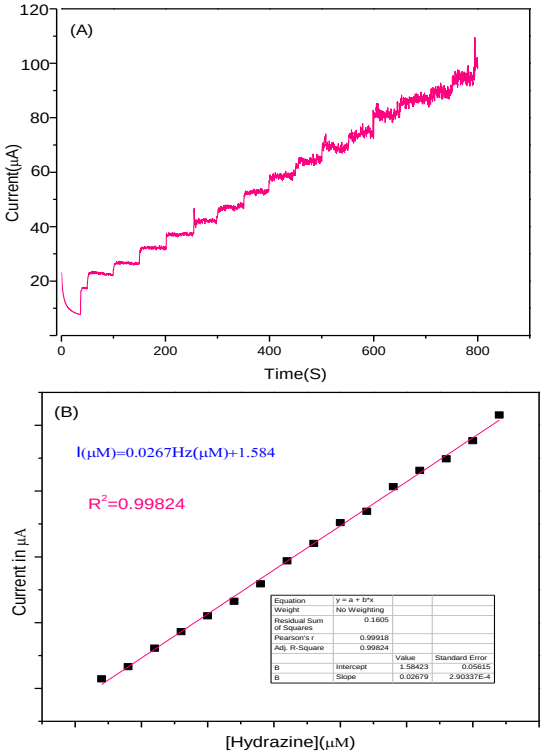

Fig 11.(A)Amperometric i-t response of ZnO/MnO_2 modified GCE during successive injection of 5µM to 90 µM of hydrazine at applied Potential of +0.48V 0.1M PBS(P^H7.4) (B) plot of peak current v/s concentration.

However by measuring CV responses for ZnO/MnO_2 modified GCE under different scan rates condition in the range 50 mvs^{-1}fig.9(A) shows linear alignment of oxidation peak of hydrazine with (10µM) each other with a constant potential .Further the oxidation the plot of oxidation peak current (ipa) V/s (scan rate)$^{1/2}$ fig.9(B) shows linear relationship between them .it is expressed by regression equation.Ipa(µA)=(49.53) $\gamma^{1/2}$ (mvs^{-1})+ 4.777 with correlation co efficient (R^2=0.99709).this declares that obtained oxidation peak associated for hydrazine (50µM) for ZnO/MnO_2/GCE modified is typically diffusion controlled electrode kinetics. Comparision of electro chemical oxidation pathway of hydrazine for modified electrodes has been previously reported.The following equations reveals that electrode reactions involved with 4 electron transfer ,at the last step gives N_2 gas.

$N_2H_4+H_2O \rightarrow N_2H_3+H_3O^{+}+ e^{-}$(slow step)

$N_2H_3+3H_2O \rightarrow N_2+3H_2O +3e^{-}$(fast Step)

$N_2H_4+4H_2O \rightarrow N_2+4H_2O+4e^{-}$(over all reaction)

It reveals slow step (1 electron)process is rate determining step followed step is 3 electron process with the nitrogen gas liberated as a product.

4.3 Amperometric Determination of hydrazine at ZnO/MnO_2 modified GCE.

In comparision with other voltametric technique amperometric measurement of i-t response at a one particular fixed potential give more sensitive and trustworthy data on sensor performance .Fig.11(A) shows detection of hydrazine by ZnO/MnO_2 modified GCE via amperometry measurement at a potential 0.48 V v/s Ag/AgCl during continuous additions from 20µM to 400 µM of PBS(0.1M) at P^H 7.4 .it reveals that upon sequential progressive addition of hydrazine for varies time intervals (50sec to 800sec)at constant potential a typical amperometric behavior was developed on the surface of the ZnO/MnO_2 modified GCE with successive increase in the oxidation current.The modified ZnO/MnO_2/GCE gives effective hydrazine detection <5 sec response time for every injection of 20 µM hydrazine .it shows modified electrode reached its steady state of oxidation .No drift in current response was observed throughout the measurement from lower concentration to higher concentration (20 µM to 400 µM).it demonstrates that modified ZnO/MnO_2/GCE has a good sensitivity and The current response for remains stable without any tendency to fluctuate for poisoning effect .Further fig 11(B). shows that calibration curve obtained for the oxidation current v/s hydrazine concentration. The amperometric current exhibit linear correlation to hydrazine concentration 20 µM-320 µM with R^2=0.9982

This can be described in equation(1) follows

$I(\mu A)= 0.02679\ [Hydrazine]+1.584$ -----→(1)

By utilizing the slope of the calibration curve 0.02679 µA μM^{-1} and surface area of electrode(0.071), current sensor sensitivity was calculated as 0.376 µA μM^{-1} it is obtained by

Sensitivity =Slope / surface area of electrode .

The limit of detection (LOD) can be calculated by applying the equation (2)

$LOD=3\sigma$ →(2)

σ=standard deviation calculated for 7 amperometric current measurement for fixed concentration was found to be 2.87 µM

Journal of Molecular Science
Journal of Molecular Science
Volume 35 Issue 3, Year of Publication 2025, Page 1237-1245
DoI-10.004687/1000-9035.2025.165

4.4 Table 1.Shows Comparitive study of modified sensor performance with previously reported sensor electrodes.

Electro chemical sensor	Method	Linear range(µM)	Limit of detection(LOD) (µM)	SensitivityµAµ M^{-1}	Reference
NG-PVP/AuNps /SPCE	AMP	2-300	0.07	1.370	25
ZNO/nafion /Au	AMP	0.8-200	0.25	0.51	26
Au Nps /GPE	AMP	25-100	3.07	---	27
Pd/C Nanofibers	AMP	---	2.9	--	28
PdNps-EDAC/GCE	DPV	5-150	1.5	0.218	29
NG-PVP/Au Nps /SPCE	SWV	2-300	0.07	1.370	30
ZnO nano rods	AMP	0.071	0.07	9.46	31
MWCNT and Chloregenic acid	AMP	---	8.0	0.0041	32
ZnO/II/Au	AMP	0.06-425	0.066	1.6	33
ZnO/MnO_2/GCE	AMP	10-700	2.87	0.376	Present work

Sensing mechanism and its role of ZnO/MnO_2 during the sensing process:

Comparison of most of the previously described electrochemical sensors for the determination of hydrazine is listed in Table () based mainly on ZnO/MnO_2 composite materials. The currently proposed ZnO/MnO_2 GCE showed improved sensitivity, low detection limit, wide range, and good stability. Especially, the current modified ZnO/MnO_2/GCE signifies enhanced sensitivity compared to other various modified electrodes of 0.218[29],1.370[30], and 0.0041[32]. By considering LOD, it also shows a lower LOD in comparison to 8.0(32) and also comparable LOD to the already reported data using 2.9[28].

4.5 Selectivity, repeatability, reproducibility of newly developed sensor:

For the application of electrochemical sensors, examination of sensor selectivity, operational stability, reproducibility, and repeatability is highly essential. Fig (12) shows certain metal anion species and bioactive molecules as common interfering species. Initially, the sensing of hydrazine was performed using ZnO/MnO_2-modified GCE with interfering species in continuously stirred 0.1 M PBS at pH 7.4 with 10 µM hydrazine concentration. The modified electrode only recorded the regular addition of hydrazine and showed no significant recording of individual concentrations of 100 µM metal ions and bioactive molecules. The notable amperometric responses were obtained only for hydrazine, and no significant response was observed for any interfering species. The result of this interfering test justifies the good selectivity behavior of the proposed modified sensor on the surface of GCE.

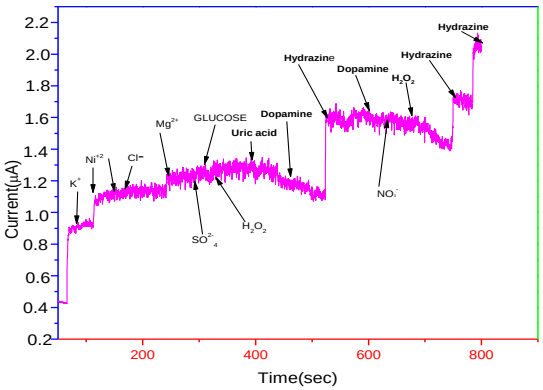

Fig.12 .The selectivity test of ZnO/MnO_2/GCE upon the addition of hydrazine (0.05mM)and interfering species KCl,$NiNO_3$,$MgSO_4$, Glucose,dopamine,Hydrazine,H_2O_2 ,(0.1mM) at 0.1M PBS (pH=7.4),at applied potential+0.46V.

The operational stability, repeatability, and reproducibility of the ZnO/MnO_2 electrode were further investigated. Hydrazine sensing with the concentration of 10 µM using five various modified electrodes gives a relative standard deviation (RSD) of ~3.5%, signifying excellent electrode reproducibility.

Repeatability tests were conducted by performing 10 regular cycle runs in 10 µM hydrazine concentration, and the acquired RSD was less than 5%. Continuous analysis of ZnO/MnO_2-modified GCE for an hour with the same hydrazine solution concluded that the (i–t) characteristic remains >95% of the initial current. Additionally, there is no decrease in sensitivity after being stored for over a month. This illustrates that the present modified sensor holds unique characteristic features for long-term stability and consistency.

4.6 Application in Real Sample Analysis:-

In order to verify the proposed method for the hydrazine sensing in practical application, real sample analysis was conducted by using tap water and bore well water by considering the standard addition method. Drinking water (surface and groundwater) may be contaminated by hydrazine from industrial wastewater treatment plant effluents. In general, hydrazine can be formed as a

Journal of Molecular Science
Volume 35 Issue 3, Year of Publication 2025, Page 1237-1245
DoI-10.004687/1000-9035.2025.165

by-product due to the conventional chlorination process, which usually applied in the wastewater treatment plant [34,36]. Therefore, the determination of hydrazine in drinking water is certainly important concerning human health and the environment. Here, three different hydrazine concentrations were added separately to the tap water and borewell water samples in 0.1 M PBS with P^H 7.4 analyzed in amperometric technique at +0.48 V applied potential using the current fabricated electrode. The real sample analytical results are Mentioned in Table 2. The results showed the acceptable recovery of hydrazine in real sample analysis, which signifies that the current sensor electrode is an excellent candidate for hydrazine determination in practical applications.

Table 2 Determination of hydrazine in tap water and Bore-well water samples by the standard addition method.

Samples	Sample code	Added(µM)	Found(µM)	Recovery (%)
Tap water	A	20	20.19	100.95
Bore-well	B	40	40.25	100.62
	C	60	59.54	99.23
	A	20	18.95	94.75
Water	B	40	40.29	100.72
	C	60	61.46	102.43

5.0 CONCLUSION:

In summary, a newly constructed hydrazine electrochemical sensor was developed through the hydrothermal method. Due to the collaborative electrocatalytic effect of both metal oxides, the presently proposed ZnO/MnO_2-modified GCE-based sensor shows reinforced achievement toward the detection of hydrazine compared with bare GCE or pure ZnO or MnO_2, and other modified electrodes that have been reported earlier.Under optimum conditions, hydrazine was detected at different concentration ranges (20 µM–800µM) with high sensitivity 0.376 µA μM^{-1} and a lower detection limit of 2.87µM. The amperometric analysis disclosed that the currently recommended hydrazine sensor established a very fast (<5 s) response with excellent long-term operational stability and repeatability. Furthermore, superior selectivity for the detection of hydrazine was achieved as proven by amperometric runs in the presence of higher concentrations of different interfering competing species. These analytical results mentioned on the synthesis, modification, and operation of the hydrazine electrochemical sensor shows that the binary composite metal oxide facilitates the construction of high-performance sensor devices.

ACKNOWLEDGEMENTS:

The Author express appreciation to siddaganga institute of technology (S.I.T) for Instrument facility and Technical support.

REFERENCES:

1. Shahid, M.M.; Rameshkumar, P.; Basirun, W.J.; Wijayantha, U.; Chiu, W.S.; Khiew, P.S.; Huang, N.M. An electrochemical sensing platform of cobalt oxide@gold nanocubes interleaved reduced graphene oxide for the selective determination of hydrazine. *Electrochim. Acta* **2018**, *259*, 606–616.
2. Troyan, J.E. Properties, Production, and Uses of Hydrazine. *Ind. Eng. Chem.* **1953**, *45*, 2608–2612.
3. Rahman, M.M.; Balkhoyor, H.B.; Asiri, A.M. Ultrasensitive and selective hydrazine sensor development based on Sn/ZnO nanoparticles. *RSC Adv.* **2016**, *6*, 29342–29352.
4. Zhao, S.; Wang, L.; Wang, T.; Han, Q.; Xu, S. A high-performance hydrazine electrochemical sensor based on gold nanoparticles/single-walled carbon nanohorns composite film. *Appl. Surf. Sci.* **2016**, *369*, 36–42.
5. Sun, M.; Guo, J.; Yang, Q.; Xiao, N.; Li, Y. A new fluorescent and colorimetric sensor for hydrazine and its application in biological systems. *J. Mater. Chem. B* **2014**, *2*, 1846–1851.
6. Guo, R.; Fang, L.; Dong, W.; Zheng, F.; Shen, M. Enhanced photocatalytic activity and ferromagnetism in Gd-doped $BiFeO_3$ nanoparticles. *J. Phys. Chem. C* **2010**, *114*(49), 21390–21396.
7. Salimi, A.; Miranzadeh, L.; Hallaj, R. Amperometric and voltammetric detection of hydrazine using glassy carbon electrodes modified with carbon nanotubes and catechol derivatives. *Talanta* **2008**, *75*, 147–156.
8. Tajik, S.; Beitollahi, H.; Hosseinzadeh, R.; Afshar, A.A.; Varma, R.S.; Jang, H.W.; Shokouhimehr, M. Electrochemical detection of hydrazine by carbon paste electrode modified with ferrocene derivatives, ionic liquid, and CoS_2 carbon nanotube nanocomposite. *ACS Omega* **2021**, *6*(7), 4641–4648.
9. Zare, H.; Habibirad, A. Electrochemistry and electrocatalytic activity of catechin film on a glassy carbon electrode toward the oxidation of hydrazine. *J. Solid State Electrochem.* **2006**, *10*, 348–359.
10. Mohammad, A.; Khan, M.E.; Alarifi, I.M.; Cho, M.H.; Yoon, T. A sensitive electrochemical detection of hydrazine based on SnO_2/CeO_2 nanostructured oxide. *Microchem. J.* **2021**, *171*, 106784.
11. Li, J.; Lin, X. Electrocatalytic oxidation of hydrazine and hydroxylamine at gold nanoparticle–polypyrrole nanowire modified glassy carbon electrode. *Sens. Actuators B* **2007**, *126*, 527–535.
12. Ivanov, S.; Lange, U.; Tsakova, V.; Mirsky, V.M. Electrocatalytically active nanocomposite from palladium nanoparticles and polyaniline: oxidation of hydrazine. *Sens. Actuators B* **2010**, *150*, 271–278.
13. Theyagarajan, K.; Kim, Y.-J. Recent developments in the design and fabrication of electrochemical biosensors using functional materials and molecules. *Biosensors* **2023**, *13*(4), 424.
14. Anantha, M.S.; Kumar, S.R.K.; Anarghya, D.; Venkatesh, K.; Santosh, M.S.; Kumar, K.Y.; Muralidhara, H.B. ZnO@MnO_2 nanocomposite modified carbon paste electrode for electrochemical detection of dopamine. *Sensors Int.* **2021**, *2*, 100087.
15. Beitollahi, H.; Tajik, S.; Garkani Nejad, F.; Safaei, M. Recent advances in ZnO nanostructure-based electrochemical sensors and biosensors. *J. Mater. Chem. B* **2020**, *8*(27), 5826–5844.
16. Singh, M.; Bhardiya, S.R.; Asati, A.; Sheshma, H.; Rai,

Journal of Molecular Science
Volume 35 Issue 3, Year of Publication 2025, Page 1237-1245
DoI-10.004687/1000-9035.2025.165

A.; Rai, V.K. Design of a sensitive electrochemical sensor based on ferrocene reduced graphene oxide/Mn spinel for hydrazine detection. *Electroanalysis* **2021**, *33*(2), 464–472.
17. Galstyan, V.; Bhandari, M.P.; Sberveglieri, V.; Sberveglieri, G.; Comini, E. Metal oxide nanostructures in food applications: Quality control and packaging. *Chemosensors* **2018**, *6*(2), 16.
18. Serov, A.; Kwak, C. Direct hydrazine fuel cells: A review. *Appl. Catal. B* **2010**, *98*(1–2), 1–9.
19. Kumar, A.; Singh, A.; Sharma, A.; Verma, R.; Kumar, A. Hydrazides as powerful tools in medicinal chemistry: Synthesis, reactivity, and biological applications. *Molecules* **2025**, *30*(13), 2852.
20. Li, H.; Wu, D.; Li, L.; Chen, X.; Zhang, W. Rapid and selective detection of hydrazine based on a fluorescent probe: Application in environmental and biological samples. *Anal. Chem.* **2020**, *92*(15), 10225–10232.
21. Zhang, Y.; Liu, Z.; Wang, Y.; Li, J.; Chen, X. Electrochemical sensors for hydrazine detection: Recent advances and future prospects. *Biosens. Bioelectron.* **2019**, *126*, 710–720.
22. Campuzano, S.; Pedrero, M.; Yáñez-Sedeño, P.; Pingarrón, J.M. Antifouling (bio)materials for electrochemical (bio)sensing. *Int. J. Mol. Sci.* **2019**, *20*(2), 423.
23. Khand, Nadir H., Amber R. Solangi, Huma Shaikh, Zia-ul-Hassan Shah, Sanoober Bhagat, Syed Tufail H. Sherazi, and Eduardo Alberto López-Maldonado. "Novel electrochemical ZnO/MnO_2/rGO nanocomposite-based catalyst for simultaneous determination of hydroquinone and pyrocatechol." *Microchimica Acta* 191, no. 6 (2024): 342.
24. Anantha, M. S.; Kumar, S. R. K.; Anarghya, D.; Venkatesh, K.; Santosh, M. S.; Kumar, K. Y.; Muralidhara, H. B. ZnO@MnO_2 Nanocomposite Modified Carbon Paste Electrode for Electrochemical Detection of Dopamine. *Sens. Int.* **2021,** *2,* 10008
25. C. Saengsookwaow, R. Rangkupan, O. Chailapakul, N. Rodthongkum, Nitrogen-doped graphene polyvinylpyrrolidone/gold nanoparticles modified electrode as a novel hydrazine sensor, Sens. Actuat. B Chem. 227 (2016) 524 532,
26. Y. Ni, J. Zhu, L. Zhang, J. Hong, Hierarchical ZnO micro/nanoarchitectures: hydrothermal preparation, characterization and application in the detection of hydrazine, CrystEngComm 12 (2010) 2213–2218,
27. M. Abdul Aziz, A.-N. Kawde, Gold nanoparticle-modified graphite pencil electrode for the high-sensitivity detection of hydrazine, Talanta 115 (2013) 214–221
28. Zhang, H.; Huang, J.; Hou, H. Electrochemical Detection of Hydrazine Based on Electrospun Palladium Nanoparticle/Carbon Nanofibers. *Electroanalysis* **2009**, *21*, 1869–1874.
29. Ahmar, H.; Keshipour, S.; Hosseini, H.; Fakhari, A. R.; Shaabani, A.; Bagheri, A. Electrocatalytic oxidation of hydrazine at glassy carbon electrode modified with ethylenediamine cellulose immobilized palladium nanoparticles. *J. Electroanal. Chem.* 2013, *690*, 96– 103,
30. Saengsookwaow, C.; Rangkupan, R.; Chailapakul, O.; Rodthongkum, N. Nitrogen-doped graphene–polyvinylpyrrolidone/gold nanoparticles modified electrode as a novel hydrazine sensor. *Sens. Actuators, B* 2016, *227*, 524– 532
31. A. Umar, M.M. Rahman, Y.B. Hahn, ZnO nanorods based hydrazine sensors, J. Nanosci. Nanotechnol. 9 (2009) 4686-4691
32. K.N. Han, C.A. Li, M.P.N. Bui, X.H. Pham, G.H. Seong Control of ZnO morphologies on carbon nanotube electrodes and electrocatalytic characteristics toward hydrazine, Chem. Commun. 47 (2011) 938-940.
33. A Salimi, L Miranzadeh, R Hallaj, Amperometric and voltammetric detection of hydrazine using glassy carbon electrodes modified with carbon nanotubes and catechol derivatives, Talanta 75 (2008) 147-156.
34. W. Sultana, S. Ghosh, B. Eraiah, Zinc oxide modified au electrode as sensor for an efficient detection of hydrazine, Electroanalysis. 24 (2012) 1869-1877.
35. Davis, W. E., II; Li, Y. Analysis of Hydrazine in Drinking Water by Isotope Dilution Gas Chromatography/Tandem Mass Spectrometry with Derivatization and Liquid–Liquid Extraction. *Anal. Chem.* **2008**, *80* (14), 5449–5453.
36. Oh, J.-A.; Shin, H.-S. Simple and Sensitive Determination of Hydrazine in Drinking Water by Ultra-High-Performance Liquid Chromatography–Tandem Mass Spectrometry after Derivatization with Naphthalene-2,3-Dialdehyde. *J. Chromatogr. A* **2015**, *1395*, 73–78.